CHAPTER - II

PLASMONS AND THEIR DAMPING IN A DOPED SEMICONDUCTOR SUPERLATTICE

The complex zeroes of dielectric response function of a doped GaAs superlattice are computed to study the frequencies and damping rates of oscillations in coupled electron-hole plasma. The real part of a complex zero describes the plasma frequency, whereas imaginary part of it yields the damping rate. Strong scattering of charge carriers from random impurity potentials in a doped GaAs superlattice gives rise to a large value of damping rate which causes over-damping of plasma oscillations of coupled electron-hole gas below q_c, a critical value of wave vector component (q) along the plane of a layer of electrons (holes). The plasma oscillations which correspond to electrons gas enter into over-damped regime for the case of weak coupling between layers. Whereas, plasma oscillations which belong to hole gas go to over-damped regime of oscillations for both strong as well as weak coupling between layers. The damping rate shows strong q-dependence for $q < q_c$, whereas, it weakly depends on q for $q \geq q_c$. The damping rate exhibits a sudden change at $q=q_c$, indicating a transition from non-diffusive regime (where collective excitation can be excited) to diffusive regime (over-damped oscillations).

2.1 Introduction

The electronic collective excitations in semiconductor superlattices have been the subject of immense theoretical and experimental research interests ever since the discovery of semi-conductor nanostructures [1-9]. Investigations were basically motivated by the potential usefulness of plasma frequency in characterisation of electronic and optical properties of a material. The collective excitation frequencies are given by the zeroes of the dielectric response function of a system. The frequencies at which dielectric response function goes to zero are complex quantities and they are functions of wave vector. The real part of a zero of dielectric function gives plasma frequency (ω_p), whereas the imaginary part of it yields damping rate (α) of a plasma oscillations. A doped semiconductor superlattice (DSSL) exhibits a strong scattering of electrons (holes) from random impurity potentials present in it. The impurity scattering causes the electrons (holes) to duffuse instead of moving ballistically [10-11]. Therefore, the plasma oscillations in a DSSL hold different states as compared to plasma oscillations in other compositional superlattices [12]. The relaxation time [τ] for single particle scattering in a DSSL has been found much shorter in comparison with the τ for a compositional superlattice where electrons (holes) are separated from ionized impurities. Small value of τ leads to a strong damping rate of

plasma oscillations, for certain wave vector values. An electron (hole) plasma mode approaches the pair continuum to meet the damping region at some critical values of the wave vector. The plasmons in a system can be said well behaved if $\omega_p \gg \alpha$. For $\omega_p \cong \alpha$ or $\omega_p < \alpha$ plasmons are not well behaved and they cannot be observed experimentally. In case of DSSL, small value of τ results in a large value of α for electron-hole coupled plasma oscillations. The condition $\omega_p \gg \alpha$ can only be acheived for higher values of in plane wave vector component (q) for a given value of out of plane wave vector component (k_z). Similar to the case of ω_p, α too is function of both q and k_z and it forms a band when it is plotted as a function of q for all possible values of k_z, The study of α, therefore, appears to be equally important as that of ω_p, in case of DSSL.

In this chapter we report a calculation of zeroes of dielectric response function, $\in(q,k_z,z)$ for GaAs-DSSL. Here, z is complex frequency. The GaAs-DSSL is modelled to be periodic array of layers consisting of electrons and holes alternatively along z-axis in dielectric host medium of dielectric constant, $\in_0$. The electrons and holes are assumed to be confined to their respective layers. The motion of an electron and of a hole in the x-y plane is assumed to be that of free particle with effective mass, m^*_e for an electron and m^*_h for hole. Harmonic oscillator wave functions are used as envelope functions to describe electron (hole) motion along z-axis. Calculation of $\in(q,k_z,z)$ involves τ which can depend on both the wave vector and frequency . We perform calculation of τ, within Born-approximation, using layered electron gas (LEG) model. Both ω_p and α are computed as the function of q for $-1 \leq \cos(k_z d) \leq 1$, where d is the period of superlattic along z-axis. Critical value (q_c) of q at which ω_p diminishes has also been computed as the function k_z for both electron and hole plasma oscillations. q_c varies from zero to a maximum value on changing cos ($k_z d$) from 1 to -1 for electron plasma, whereas q_c shows weak k_z -dependence for a hole plasma. Also, q_c is much higher for hole plasma oscillations as compared to that for electron plasma oscillations. The chapter is organized into four sections. Formalism of $\in(q,k_z,z)$ and τ is given in section 2.2 The computed results are discussed in section 2.3. Our work is then summarized in section 2.4

2.2 Formalism

The GaAs DSSL consists of one layer of electrons and one layer of holes in a unit cell. There exist electron - electron, hole-hole and electron-hole interactions which give rise to coupled electron-hole plasma oscillations The $\in(q,k_z,z)$ therefore consists of intralayer interaction terms (which involve

electron-electron and hole-hole interactions) and interlayer interaction terms representing electron-hole interactions. The $\in(q,k_z,z)$ for intrasubband transitions in a GaAs-DSSL is given by [13]

$$\in(q,k_z,z)=\left[1-V_qP_{ee}\left\{H_{ee}-F_{ee}(1-W_{ee})\right\}\right]x$$
$$\left[1-V_qP_{hh}\left\{H_{hh}-F_{hh}(1-W_{hh})\right\}\right]-V_q^2P_{ee}P_{hh}F_{eh}F_{he}W_{eh}W_{he}. \qquad (2.1)$$

The first term on the rhs of (2.1) is contributed by intralayer interactions, whereas second is given by interlayer interactions. Further, first term consists of two square brackets. The terms under one of the brackets are contributed by electron-electron interactions, whereas those under other brackets are contributed by hole-hole interactions. The $V_q=2\pi e^2/q\in$ and $W_{ij}(q,k_z)$ (with i and $j\equiv e,h$) is given by [13]

$$W_{ij}(q,k_z)=\frac{\exp(-q|R_{ij}|)\exp(ik_zd)}{\exp(ik_zd)-\exp(-qd)}+\frac{\exp(q|R_{ij}|)\exp(-qd)}{\exp(-ik_zd)-\exp(-qd)}, \qquad (2.2)$$

where $W_{ij}(q,k_z)\equiv W_{ij}(q,-k_z)\equiv W^*_{ij}(q,k_z)$ and $|R_{ee}|\equiv|R_{hh}|=0$. The matrix elements $H_{ij}(q)$ are defined as [13]

$$H_{ij}(q)=\int_{-d_i/2}^{d_i/2}dt\int_{-d_j/2}^{d_j/2}dt'\exp(-q|t-t'|\psi_i(t)\psi_j(t'). \qquad (2.3)$$

Here $\psi_{ij}(t)$ is the product of two envelope functions. The $F_{ij}(q)$ are given by Eq.(2.3) on replacing $q|t-t'|$ by q(t-t'). We assume that only ground sub-band is filled and it produces intrasubband plasma oscillaitons, for both electrons and the holes. The $H_{ij}(q)$ and $F_{ij}(q)$ are evaluated using the envelope functions

$$\psi_{ij}=|\phi_j|^2, \qquad (2.4)$$

where ϕ_j are the harmonic oscillator wave functions, which can be given by

$$\phi_j=N^n\exp(-\beta_jz^2/2)H^n(\beta_j) \qquad (2.5)$$

with

$$N^n=(\beta_j/2^n\sqrt{n!n}), \qquad (2.6)$$

where β_j is defined as

$$\beta_j = \left[\frac{4\pi e^2 m_j^* N_{D/A}}{\hbar \varepsilon_0}\right]^{1/4}. \tag{2.7}$$

On performing integration on equation (2.3) with the use of equations (2.4) and (2.5) we obtain

$$H_{jj}(q) = \exp\left(\frac{q^2}{2\beta_j^2}\right) - \left(\frac{\sqrt{2}}{\sqrt{\pi}}\right)\left(\frac{q}{\beta_j}\right)\exp\left(\frac{-q^2}{2\beta_j^2}\right) \tag{2.8}$$

and

$$F_{jj} = \exp\left[\frac{q^2}{4}\left(\frac{1}{\beta_j} + \frac{1}{\beta_j^2}\right)\right]. \tag{2.9}$$

$N_{D/A}$ is the number of donors/acceptors per unit volume. The P_{ee} and P_{hh} are the non-interacting polarizabilities for two-dimensional (2D) electron and hole gases, respectively. For intrasub-band transitions, P_{ee} and P_{hh} are given by [14].

$$P_{jj}(q,z) = \frac{n^2_{sj} q}{m^*_j[(q^2 v^2_{fj}/2) - z[(z + i\gamma_j(q))]}, \tag{2.10}$$

where v_{fj} and $\gamma_j(q)$ are Fermi velocity and single particle damping for an electron (a hole), respectively .The n_{sj} is the number of electrons (holes) per unit area. The $\gamma_j(q)$ is the inverse of τ_j which for electron (hole) scattering from random impurity potential, within Born-approximation, is given by [15]

$$\gamma_j(q) = \frac{2\pi n_{D/A}}{\hbar}\int \frac{d^2k}{4\pi^2}|V(k'-k)|^2(1-\cos\theta)\delta(\in_{k'} - \in_k), \tag{2.11}$$

where $n_{D/A}=N_{D/A}\,d$ and θ is the angle between $\vec{k}$ and $\vec{k}'$ The $\vec{k}$ and $\vec{k}'$ are wave vector component in x-y plane. $\in_k$ is the single particle energy eigenvalue and *V(k'-k)* is screened random impurity potential . We solve Eq. (2.11) by taking LEG model based expression for *V(k'-k)* [14] to obtain

$$\gamma(q)=\frac{8n_{D/A}ze\pi^2\hbar C_j}{m_j^*(qa_j^*)^2}\left[\frac{1+F(q)(1/qa_e^*+1/qa_h^*)+g(q)}{\left\{1+R^2(q)+2R(q)\coth(qd)\right\}^{1/2}}-\sinh(qd/2)\right]^2, \quad (2.12)$$

where

$$R(q)=2\left[\frac{1}{qa_e^*}+\frac{1}{qa_h^*}\right]+\frac{4F(q)}{q^2a_e^*a_h^*}, \quad (2.13)$$

$$g(q)=\cosh(qd/2)+\sinh(qd/2)R(q) \quad (2.14)$$

and

$$F(q)=\frac{(\cosh(qd)-1)}{\sinh(qd)} \quad (2.15)$$

The z_e represents the charge on an impurity and $a_j^*=(\varepsilon_0\hbar^2/m_j^*e^2)$ is effective Bohr radius and C_j is a constant introduced in an empirical manner to obtain right order of values of $\gamma(0)$ which is comparable with the value of damping constant estimated from experimentally measured values of electron (hole) mobility in DSSL [16]. We continue to discuss our results in the next section.

2.3 Results and discussion

Equation $\in(q,k_z,z)=0$ is solved for z as a function of q and k_z using Eqs.(2.2) to (2.15). Simplification of $\in(q,k_z,z)=0$ yields a IVth order equation in z, which has no real root. All four roots are complex. An analytical solution of $\in(q,k_z,z)=0$ is not possible. We solved $\in(q,k_z,z)=0$ numerically using iterative method of finding complex zeroes of a function. For computation of our results, we modelled GaAs-DSSL in terms of the following values of parameters [13]: $\in_0=12.5$, $d_e=600$ Å, $d_h=500$ Å, $d_i=100$ Å, $n_{se}\equiv n_{sh}=10^{12}$ cm^{-2}, $m_e^*=0.07\ m_e$, $m_h^*=0.7\ m_e$, $n_D=5\times10^{12}$ cm^{-2} and $n_A=2\times10^{12}$ cm^{-2}, $C_e=1.742\times10^{-2}$ and $C_h=3.9213\times10^{-4}$. The d_e, d_h and d_i are the widths of an electron layer, a hole layer and an undoped layer between an electron layer and a hole layer, respectively. The $d=d_e+d_h+2d_i$. Our computed ω_p (real part of z-values at which $\in(q,k_z,z)$ goes to zero) are plotted as a function of qd for $-1\le\cos(k_zd)\le1$ in figure 2.1. The figure shows two bands of ω_p for coupled electron-hole plasma oscillations. The upper band which corresponds to electron plasma frequencies is wide,

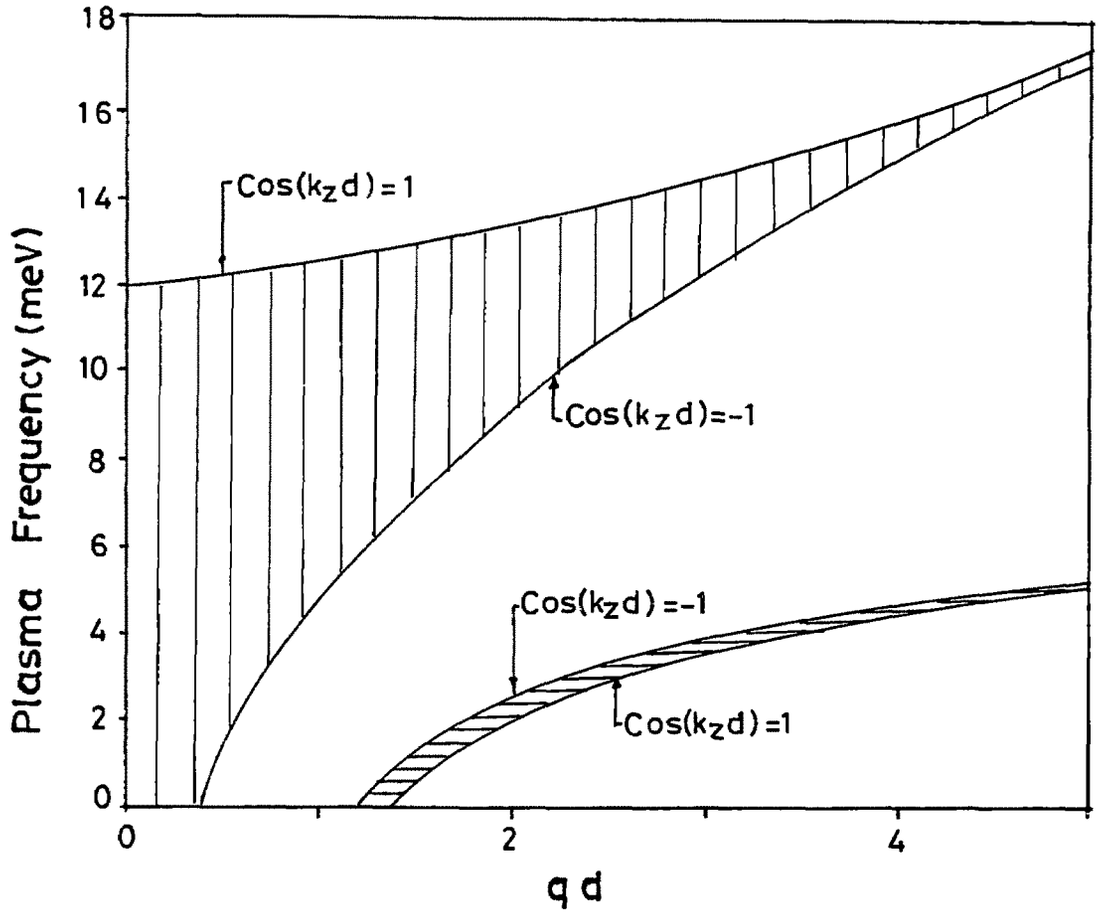

Fig. 2.1 The coupled electron-hole plasma frequencies as a function of qd.

whereas lower band which represents the hole plasma frequencies is narrow. Also, hole plasma frequencies are much softer as compared to the electron plasma frequencies. The lower edge (which occurs at $\cos(k_z d) = -1$) of electron plasma band varies approximately as $(q^2 - q^2_c)^{1/2}$ and it disappears at $q=q_c$. Whereas, upper edge (which correspond to $\cos(k_z d)=1$) remains nonzero for all values of q and it becomes almost independent of q for small q-values. Plasma modes in lower band, which correspond to hole gas, disappear as $(q^2-q^2_c)^{1/2}$ at $q=q_c$ for all possible values of $\cos(k_z d)$ as it can be seen from the figure 2.1. Also, upper edge of hole plasmon band corresponds to $\cos(k_z d) = 1$, whereas lower edge of it belongs to $\cos(k_z d) = -1$. The $\cos(k_z d)=1$ also corresponds to $d \to 0$ limit in which layers of charge carries strongly interact with each other and the DSSL behaves like a two component 3D isotropic free charge carrier gas. On the other hand, $\cos(k_z d) = -1$ represents the case of finite d which can be very large. For large value of d, there is weak interlayer coupling and each layer in DSSL behaves independent of others. In weak coupling case, plasma oscillations are essentially of 2D nature. We thus notice that electron gas gives higher plasma frequency in strong coupling limit, whereas hole gas yields higher plasma frequency for weak coupling case of a DSSL. The bands of both the electron plasma as well as hole plasma get narrower on increasing qd.

The asymptotics of our results can be obtained for the case of weak coupling between the layers ($\cos(k_z d) = -1$). For weak coupling case ($\cos(k_z d) = -1$), second term on right hand side of Eq. (2.1), which represents coupling between electron plasma and hole plasma oscillations, is negligibly small and it can be dropped. Solution of Eq.(1) then yields.

$$z_j(q,\pi/d) = \left[\left\{\frac{q^2 v_{Fj}^2}{2} + \omega^2_{oj} T_{jj}(q,\pi/d)\right\} - (\gamma_j^2(q)/4)\right]^{1/2} - i\gamma_j/2, \qquad (2.16)$$

where

$$\omega^2_{oj} = \frac{2\pi e^2 n_{sj} q}{m^*_j \in_0} \qquad (2.17)$$

and

$$T_{jj}(q,\pi/d) = H_{jj}(q) - F_j(q)\left[1 - W_{jj}(q,\pi/d)\right]. \qquad (2.18)$$

For small q-values, $H_{jj} \cong F_{jj} \cong 1$ and $T_{jj}(q,\pi/d) \cong qd/2$, which gives rise to

$$z_j(q,\pi/d) \cong \frac{1}{2}\omega_{pj} d\left[(1+a_j^*/d)^2(q^2-q_{cj}^2)\right]^{1/2} - i\gamma_j(q)/2, \qquad (2.19)$$

where $\omega_{pj} = (4\pi n_{sj} e^2/m_j^* \in_0)^{1/2}$ is 3D plasma frequency. The q_{cj} is defined as

$$q_{cj} d = \gamma_j(0)/\omega_{pj}(1+a_j^*/d)^{1/2}. \qquad (2.20)$$

As is obvious, non-zero real part of $z_j(q,\pi/d)$ exists for $q > q_{cj}$. The q_{cj} is determined by γ_j, n_{sj} and m_j^*, as can be seen from Eq.(2.12). Computation of Eq. (2.20) gives $q_{ce}d$=0.4294 and $q_{ch}d$= 1.2934, which coincided with the values shown in figure 2.2. Our computed q_c values for both electron and hole plasma oscillations using Eq. (2.1) are plotted as the function of cos ($k_z d$) in figure 2.2. It can be seen from the figure that q_c varies from zero (at cos ($k_z d$)=1) to maximum value (at cos(k_zd) = -1) for electron plasma oscillations. The q_c shows a small variation on changing cos ($k_z d$) from 1 to -1 for hole plasma oscillaitons. The $q_c d$ is found to be roughly proportional $(k_z d)^{1/2}$ for electron plasma oscillations.

Figure 2.3 (a) shows the plot of α_h (α for hole plasma oscillations) as a function of qd for $-1 \le \cos(k_z d) \le 1$. Similar to the case of ω_p for plasma oscillation, upper edge of α_h band belongs to cos($k_z d$) = -1, whereas lower edge of it corresponds to cos($k_z d$) = 1. The α_h forms a narrow band and exhibits a sudden change at $q = q_c$. The sudden change in α_h can be well understood from Eq (2.19) whcih clearly shows that for $q < q_c$, both terms on right hand side are imaginary giving rise to purely imaginary value of $z_j(q,\pi/d)$ For $q<q_c$, α_h strongly depends on q, whereas for $q>q_c$, α_h weakly depends on q. It is to be noted that for $q \le q_c$ electron (hole) system enters into a diffusive regime where plasma oscillations are overdamped to yield $\omega_p = 0$. The transitions from diffusive regime to non-diffusive regime, which occurs at $q = q_c$, can clearly be seen in figure 2.3(a) and form Eq. (2.19). It can be inferred from figure 2.3(a) and Eq. (2.19) that the value of τ_h in diffusive regime is much smaller than its value in non-diffusive regime, suggesting that the mean free path in diffusive regime is smaller than that in non-diffusive regime. Also, the mean free path in diffusive regime becomes much smaller than the width of a layer It can also be seen from figure 2.3(a) that the α_h band tends to saturate as q approaches zero. The coupling between electron and hole plasma oscillations, which

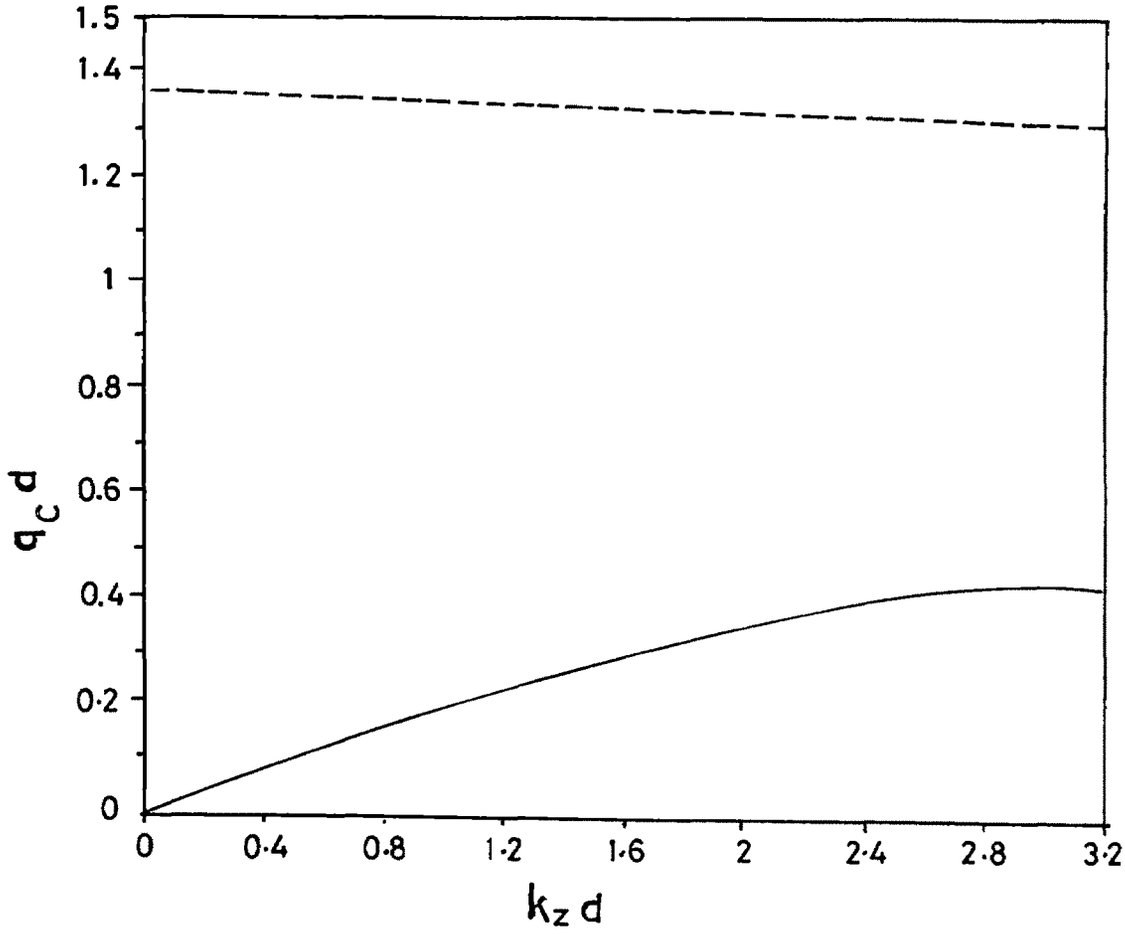

Fig. 2.2 Critical q-values as a function of $k_z d$ for coupled electron-hole plasma oscillations. The solid curve corresponds to electron plasma, whereas dash-dash curve corresponds to hole plasma oscillations.

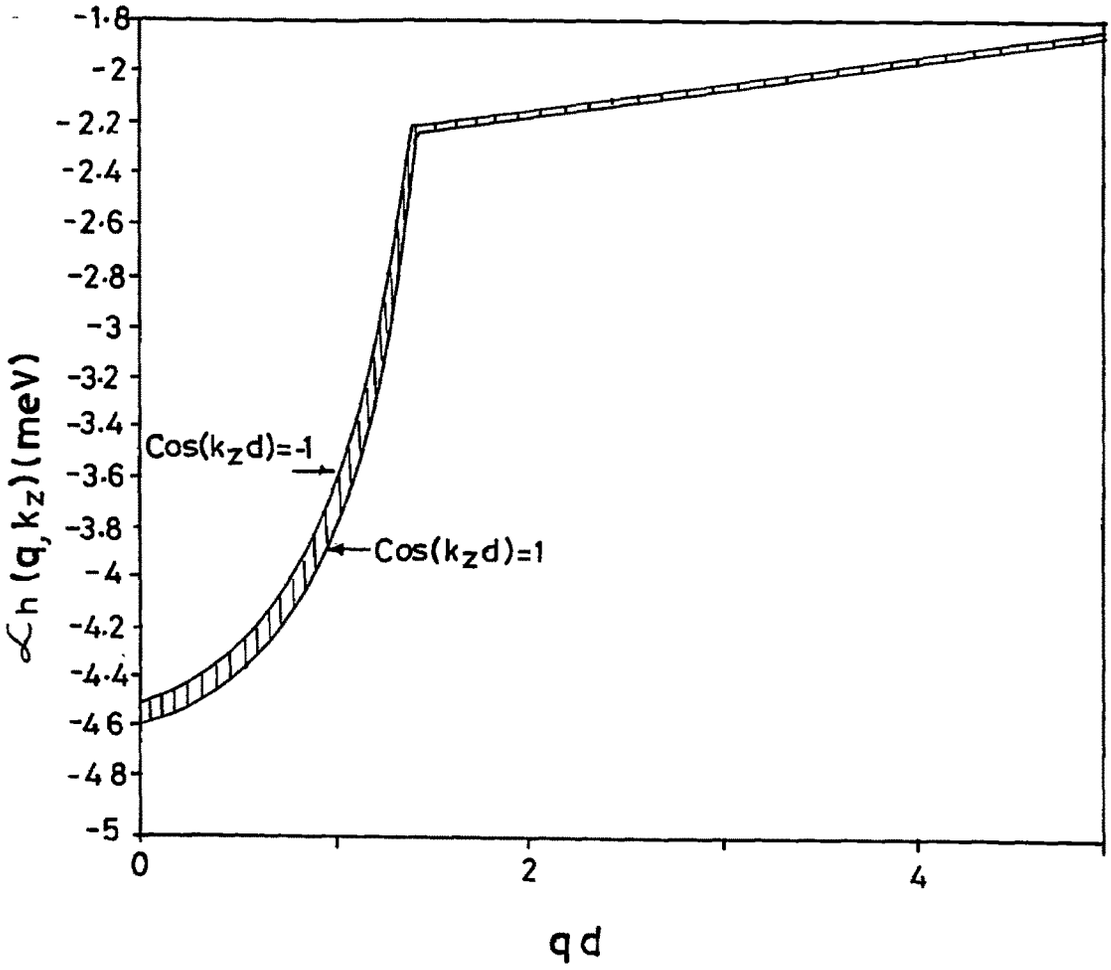

Fig. 2.3 (a) The plot of damping rate for hole plasma oscillations as a function of qd for - $1 \leq \cos(k_z d) \leq 1$.

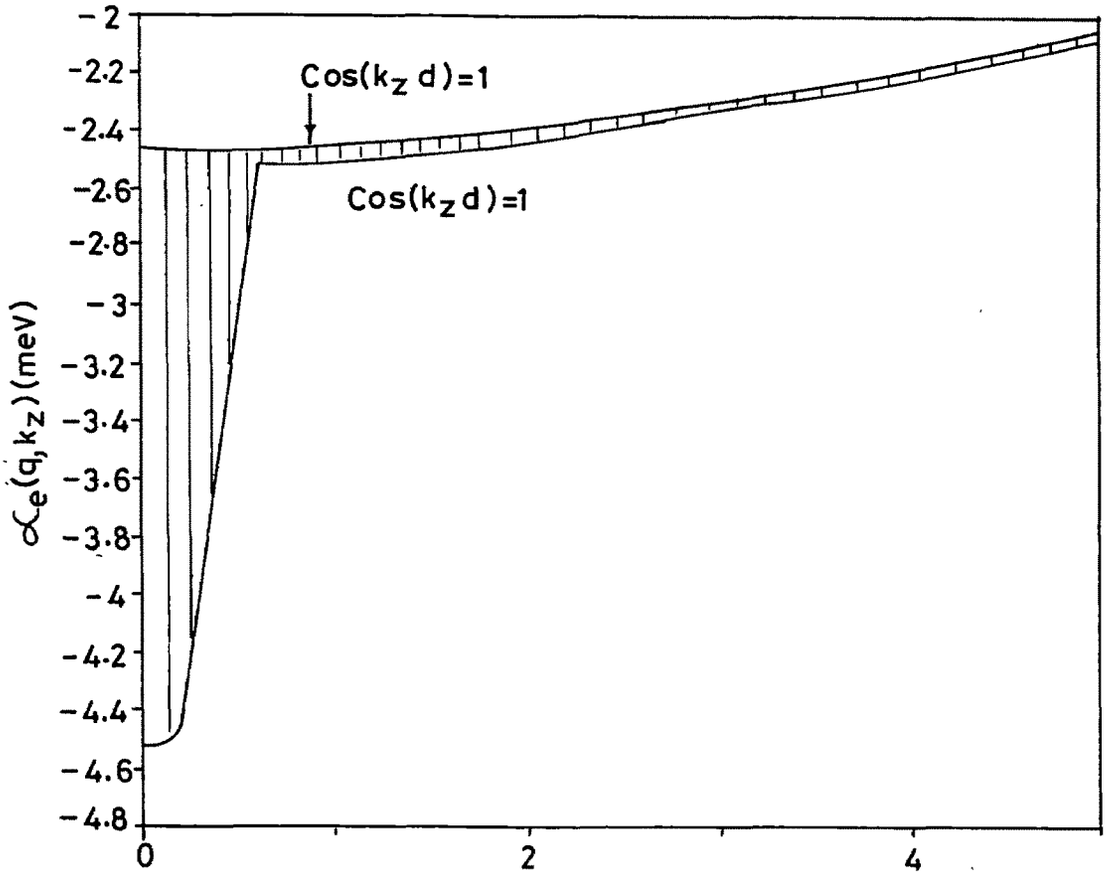

Fig.2.3 (b) Damping rate of electron plasma oscillations is plotted as a function of qd for $-1 \leq \cos(k_z d) \leq 1$.

appear through third term on the right hand side of Eq. (2.1), make a significant contribution to α_h, as is obvious from figure 2.3 (a).

The computed α_e (α for electron plasma oscillations) is plotted as a function of qd, for $-1 \leq \cos(k_z d) \leq 1$, in figure 2.3(b). Similar to α_h, the α_e also forms a narrow band showing upper edge at $\cos(k_z d) = 1$ and lower edge at $\cos(k_z d) = -1$. The behaviour of α_e is similar to that of α_h and α_h is roughly equal to α_e for $q \geq q_c$. At $q = q_c$, a sudden change can be seen in lower edge (which corresponds to the case of weak coupling between the layers) of α_e. This can also be seen from Eq. (2.19). However, the upper edge of α_e (which corresponds to the case of strong coupling between the layers does not show a sudden decrease at $q = q_c$, suggesting that the electron plasma oscillations never enter into the over-damped regime and they remain well behaved at all q-values, for the case of strong coupling between the layers. The electron plasma modes for the case of $\cos(k_z d)$ close to -1 enter into the over damped regime of plasma oscillations on lowering the q, as it can seen from figure 2.3(b) and Eq.(2.19). The α for $q < q_c$ shows stronger k_z-dependence as can be seen from figure 2.3(b). It does happen due of stronger k_z-dependence of first term of right side of Eq.(2.19), which becomes imaginary for $q < q_c$.

2.4 Summary

In conclusion, we present a calculation of complex zeroes of $\in(q, k_z, z)$ to study the plasma oscillations and their damping in GaAs-DSSL. Plasma oscillations enter into over-damped regime for $q < q_c$ for a given value of $\cos(k_z d)$. A sudden change in α at $q = q_c$ is found, which describes a transition from non-dfiffusive to diffusive regime of plasma oscillations. The α-values are much larger in diffusive regime as compared to those in non-diffusive regime.

References

[1] J. J. Quinn, G Eliason and P. Hawrylak, *Spatial dispersion in solids and plasmons*, edited by P. Halevl, (Elsevier Science Publishers B V ,1992) ch. 4, p. 243.

[2] D. Olego, A. Pinczuk, A. C. Gossard and W. Weigmann, Phys. Rev. **B25**, 7867 (1982).

[3] J. K. Jain and P. B. Allen, Phys. Rev. Lett. **54,** 947 (1985).

[4] S. Das Sarma and A. Madhukar, Phys. Rev. **B23**, 805 (1981).

[5] R. E. Camley and D. L. Mills, Phys. Rev. **B29**, 1695 (1984).

[6] P. Hawrylak, J. Wu and J. J. Quinn, Phys. Rev. **B32**, 5169 (1985).

[7] S. Katayama and T. Ando, J Phys. Soc. Jpn **54**, 1615 (1985)

[8] N. Tozor and C. Zhang, Phys. Rev. **B29** , 1050 (1986).

[9] A. C. Sharma and A. K. Sood, J. Phys. . Cond. Matt. **6,** 1553 (1994).

[10] G. F. Giulinai and J. J. Quinn, Phys. Rev. **B29**, 2321 (1984).

[11] S. Das Sarma and E. H. Hwang, Phys. Rev **B54,** 1936 (1997).

[12] S. Rudin and T. L. Reinecke, Phys. Rev. **B54**, 2791 (1995).

[13] A. C. Sharma and R. Sen. J. Phys. . Cond. Matt. **7**, 9551 (1995).

[14] A. C. Sharma, Solid State Commun. **95**, 569 (1995).

[15] T. Ando, A. B. Fowler and F. Stern, Rev. Mod. Phys. **54**, 437 (1982).

[16] Gottfried H Dohler, *The technology and physics of molecular beam epitaxy* edited by E H C Parker (New York, Plenum, 1985) p.233.